

KIF1A is the primary anterograde motor protein required for the axonal transport of dense-core vesicles in cultured hippocampal neurons

K.Y. Lo^{a,1}, A. Kuzmin^{a,1}, S.M. Unger^a, J.D. Petersen^{b,2}, M.A. Silverman^{a,*}

^a Department of Biological Sciences, 8888 University Drive, Simon Fraser University, Burnaby, British Columbia, Canada V5A 1S6

^b Junegers Center for Neurosciences Research, Oregon Health & Science University, Portland, OR 97239, USA

ARTICLE INFO

Article history:

Received 12 October 2010

Received in revised form 9 December 2010

Accepted 5 January 2011

Keywords:

Dense-core vesicle
Axonal transport
Neuropeptide
Hippocampal neuron
KIF1A
Bidirectional transport

ABSTRACT

Dense-core vesicles (DCVs) are responsible for transporting, processing, and secreting neuropeptide cargos that mediate a wide range of biological processes, including neuronal development, survival, and learning and memory. DCVs are synthesized in the cell body and are transported by kinesin motor proteins along microtubules to pre- and postsynaptic release sites. Due to the dependence on kinesin-based transport, we sought to determine if the kinesin-3 family member, KIF1A, transports DCVs in primary cultured hippocampal neurons, as has been described for invertebrate neurons. Two-color, live-cell imaging showed that the DCV markers, chromogranin A-RFP and BDNF-RFP, move together with KIF1A-GFP in both the anterograde and retrograde directions. To demonstrate a functional role for KIF1A in DCV transport, motor protein expression in neurons was reduced using RNA interference (shRNA). Fluorescently tagged DCV markers showed a significant reduction in organelle flux in cells expressing shRNA against KIF1A. The transport of cargo driven by motors other than KIF1A, including mitochondria and the transferrin receptor, was unaffected in KIF1A shRNA expressing cells. Taken together, these data support a primary role for KIF1A in the anterograde transport of DCVs in mammalian neurons, and also provide evidence that KIF1A remains associated with DCVs during retrograde DCV transport.

Crown Copyright © 2011 Published by Elsevier Ireland Ltd. All rights reserved.

1. Introduction

Secreted signaling molecules, such as chemical neurotransmitters and signaling peptides, are released into the synaptic cleft from either small, clear synaptic vesicles (SVs) or large, dense-core vesicles (DCVs). SVs are filled with classical neurotransmitters locally at presynaptic release sites. By contrast, DCVs are formed and filled with signaling peptide cargos in the cell body, and then travel long distances into the axon and dendrites to pre- and postsynaptic sites. During transit, DCV neuropeptide contents are processed and then released upon stimulation [28]. A wide range of biological processes is facilitated by DCV cargos, including neuronal survival, development, learning and memory [5]. For example, brain-derived neurotrophic factor (BDNF), a neuropeptide transported in DCVs, is required for neuronal development, both at the

level of circuit development in the brain and synaptic maturation and function [36]. In the axon, DCVs must travel extremely long distances, emphasizing the need for active cytoskeletal transport and microtubule-based motors such as kinesin family members and dynein [37,4,21]. Despite the importance of DCVs in neuronal physiology, little is known regarding the motors required for their axonal transport.

Over 45 kinesins have been identified in the mammalian genome. As motor-cargo interactions are very specific [13], these motors must distinguish among a multitude of cellular cargos (or vice versa) for efficient transport. Previous work has shown that in *Drosophila* and *C. elegans*, the homolog of mammalian KIF1A, *unc-104*, is required for axonal transport of DCVs. Mutant animals lacking UNC-104 showed transport and localization defects of the DCV cargos, including atrial natriuretic factor (ANF), IDA-1, and critical neuropeptide processing enzymes [37,4,16]. Co-immunoprecipitation studies in mouse brain suggest a conserved role of KIF1A in the transport of DCVs in mammals [24,3]. However, until now, no functional data exists demonstrating the reliance of DCV transport on KIF1A in mammalian neurons. Through the use of live-cell, two-color imaging of fluorescently tagged KIF1A and DCV marker proteins in axons and shRNA technology, we demonstrate that KIF1A is the primary motor responsible for fast axonal transport of DCVs in primary cultured hippocampal neurons. Additionally, we show that KIF1A, an anterograde motor, co-transport

Abbreviations: BDNF, brain-derived neurotrophic factor; ChrA, chromogranin A; DIV, days *in vitro*; DCV, dense-core vesicle; GFP, enhanced green fluorescent protein; NPY, neuropeptide Y; RFP, monomeric red fluorescent protein; TfR, transferrin receptor.

* Corresponding author. Tel.: +1 778 782 3647; fax: +1 778 782 3496.

E-mail address: masilver@sfu.ca (M.A. Silverman).

¹ These authors contributed equally to this work.

² Present address: Centre National de la Recherche Scientifique UMR 5091, Physiologie Cellulaire de la Synapse, Université Bordeaux, Bordeaux, France.

with DCVs that move in the retrograde direction, indicating that KIF1A can remain associated with DCVs as cargo. More generally, these data contribute to the understanding of molecular mechanisms of transport in neurons, an area of intensive investigation in the context of basic nerve cell biology, as well as synaptic plasticity and neurodegeneration [29].

2. Experimental procedures

2.1. Hippocampal cell culture and expression of transgenes

Primary cultures of dissociated neurons from rat embryonic day 18 (E18) hippocampi were prepared as previously described [17]. Plasmids were transfected into neurons after 7 DIV and allowed to express for 24–48 h before imaging. Lipofectamine 2000 (Invitrogen) was used to transfect cells with 1 μ g of each plasmid, as described by Sampo et al. [27]. For immunoblot analysis of KIF1A protein levels, freshly dissociated E18 hippocampal neurons were transfected with shRNA plasmids by electroporation, using the Nucleofector II electroporator (Amaxa Inc.), according to Kaech and Banker, [17], and allowed to express the plasmids for 48 h. Prior to protein extraction, one coverslip from each condition was assessed for transfection rate by counting the proportion of GFP-expressing cells, which was typically in the range of 60–75%.

2.2. Constructs

shRNA sequences directed against either rat or mouse KIF1A mRNA were chosen using the Dharmacon siDesign Center (Thermo Scientific). The rat KIF1A RNAi sequence encompassed base pairs (bp) 1689–1709 (5'-TACCTATGTGAACGGCAAGAA-3'; Genbank XM.001070204); control mouse KIF1A RNAi encompassed bps 1842–1862 (5'-CACATATGTCAACGGCAAGAA-3'; Genbank NM.008440). shRNA sequences were followed by the reverse complement (underlined), separated by a linker containing an EcoRV site. To facilitate cloning, an HpaI site was incorporated at the 5' end, and an XhoI site at the 3' end. The sequence 5'-**AACTACCTATGTGAACGGCAAGAATTGATATCCGTTCTTGCCGTTACATAGGTATTTTC**-3', containing the rat KIF1A RNAi sequence, and the sequence 5'-**AACCACATATGTCAACGGCAAGAATTGATATCCGTTCTTGCCGTTGACATATGTGTTTC**-3', containing the mouse KIF1A RNAi sequence (restriction sites in bold), and their respective complements, which contain a 5' phosphate, were ordered from Integrated DNA Technologies (Iowa, USA). Complementary strands were annealed and cloned into the pLentilox-GFP vector containing two promoters: one for the expression of GFP, the other for the shRNA.

Several plasmids were kindly donated from the following laboratories: GW1-KIF1A-GFP; Dr. E. Kim, KAIST, Korea; pcDNA3-ChrA-RFP, Dr. L. Taupenot, NIH, USA; mitochondrial targeted eYFP, Dr. G. Rintoul, Simon Fraser University, Canada.

2.3. Immunoblotting and immunocytochemistry

Protein levels were assessed by lysing control and shRNA expressing cells in 200 μ l of phosphate buffered saline and HALT protease inhibitor cocktail (Pierce Protein Research Products). Protein samples were sonicated and then heated in Laemmli buffer to 100 °C for 5 min. Proteins were quantified using a BCA protein assay kit (Pierce). 5 μ g of each protein were separated on a 10% SDS polyacrylamide gel. After transferring the gel to PVDF, the membrane was probed with a monoclonal anti-KIF1A antibody (BD Biosciences; 1:500) and a monoclonal anti- α -tubulin antibody (Sigma; 1:2000). Bands were visualized with goat anti-mouse-HRP secondary antibody (BioRad; 1:30,000) and SuperSignal West

Femto Maximum Sensitivity Substrate (Pierce) on autoradiography film. Relative protein amounts were quantified from scanned images of autoradiographs using ImageJ (National Institutes of Health).

To confirm protein expression of myc-RNAi resistant KIF1A, immunocytochemistry was performed as described in Kwinter et al. [21] using a polyclonal anti-myc (Sigma) primary antibody (1:250) and donkey anti-rabbit Cy5 (Jackson Immunoresearch Labs) secondary antibody (1:500).

2.4. Imaging

All single color imaging, typically 200 frames, was recorded by the 'stream' acquisition module in *MetaMorph*, as described in Kwinter et al. [21]. For two-color imaging, typically 30 exposures of 200 ms for each wavelength were taken alternately with appropriate, spectrally distinct filters controlled by the 'multi-dimensional acquisition' module in *MetaMorph*. Still images were obtained with a 20 \times 0.6 NA objective (Leica Microsystems, Germany).

2.5. Data analysis

All recordings were processed using *MetaMorph* to generate a time-distance graph for each video with the 'kymograph' function, as described in [21]. DCV flux was measured as the distance of DCV run lengths in μ m, standardized by the length of imaged axon and filming duration (μ m \times min): $\sum_{i=1}^n d_i / (l \times t)$ where d is the individual DCV run lengths (μ m), l is the length of axon observed (μ m) and t is the duration of filming, as described in [21]. Co-transport events were assessed by counting and comparing the traces on kymographs generated from two-color movies. Because of the delay in image acquisition, only unambiguous, continuous lines present in both kymographs were scored. A one tailed Student's t -test, using equal or unequal variance based on F -tests, was used to determine significance in pair wise comparisons of control and experimental conditions in Microsoft *Excel* and *SPSS*.

3. Results

If the location and movements of two labeled proteins are identical – that is, they start together, travel at the same rates, and stop together – it is likely they reside on or in the same organelle. To determine if KIF1A co-transport with DCVs, KIF1A-GFP was co-expressed with either BDNF-RFP or ChrA-RFP in primary cultured hippocampal neurons. Axonal transport of each DCV marker and KIF1A-GFP was then examined by two-color, live-cell imaging in cells where the orientation of the axon in relation to the cell body was unambiguous (Fig. 1). The degree of co-transport in the axon was determined by comparing pairs of kymographs generated for each fluorescently tagged protein. BDNF and ChrA are co-packaged in DCVs ([8] and [Supplementary movie 1](#)), and demonstrated similar transport dynamics; thus the transport data for these two DCV markers are pooled in Fig. 1D. The percentage of KIF1A co-transporting with DCV markers was $68.6 \pm 3.1\%$ in the anterograde direction and $64.6 \pm 3.1\%$ ($n=32$ axons) in the retrograde direction. The percentage of DCV markers co-transporting with KIF1A was $59.0 \pm 3.7\%$ in the anterograde direction and $54 \pm 3.7\%$ ($n=32$ axons) in the retrograde direction (Fig. 1; [Supplementary movies 2 and 3](#)). These results indicate that in the axon, not only do KIF1A and DCVs move in tandem, but they do so almost equally in both the anterograde and retrograde direction. As an alternate approach to demonstrate the colocalization of endogenous KIF1A with BDNF or ChrA, immunofluorescence staining using commercially available antibodies was used. However, the pattern and intensity of non-specific staining was similar in appearance to the expected

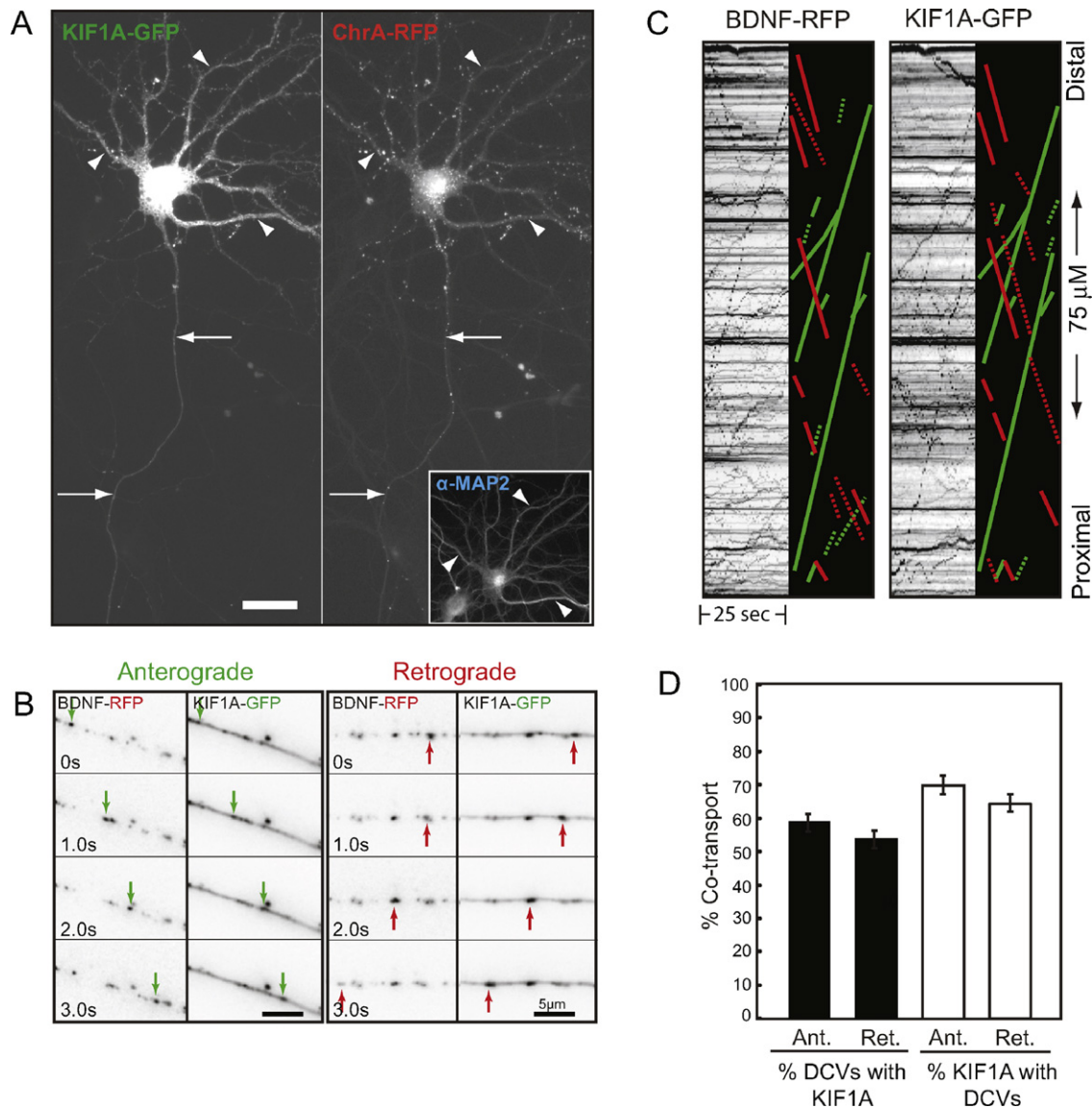


Fig. 1. KIF1A and the dense-core vesicle cargos, BDNF and chromogranin A, undergo bidirectional co-transport in primary cultured hippocampal neurons. (A) 8 DIV neurons were first analyzed by near-simultaneous, two-color live-imaging of KIF1A-GFP and ChrA-RFP, and then fixed and stained with an antibody against MAP2 (inset) to retrospectively confirm axonal (arrows) and dendritic (arrowheads) morphology. Scale bar: 25 μ m. (B) A series of frames taken from a movie of near-simultaneous, two-color imaging of BDNF-RFP and KIF1A-GFP in the axon. Particles containing BDNF-RFP and KIF1A-GFP are observed moving together in both anterograde (green arrow) and retrograde (red arrow) directions (Supplementary movies 2 and 3). (C) Example kymographs generated from near-simultaneous, two-color imaging of BDNF-RFP and KIF1A-GFP. Lines with positive slopes indicate anterograde transport events; lines with negative slopes indicate retrograde transport events. Co-transport events are distinguished with solid green (anterograde) and red (retrograde) lines; dashed lines are single transport events. (D) Quantification of co-transport events was tallied by identifying lines of similar position, slope, and length on kymographs generated from two-color movies of DCV markers and KIF1A.

structures; thus, although we find overlapping staining, the results are inconclusive.

To determine if KIF1A has a functional role in axonal transport of DCVs, the transport of BDNF-RFP or another marker of DCVs, neuropeptide Y (NPY-mCherry) [21], was imaged in rat neurons co-expressing shRNA against KIF1A. In knockdown cells, KIF1A protein levels were reduced by $70 \pm 3\%$, as assessed by immunoblotting (Fig. 2). Similar to BDNF and ChrA, NPY and BDNF are co-packaged in DCVs [21,33], and demonstrated similar transport dynamics. Thus, the transport data for these markers are pooled in Table 1. Cells in which KIF1A was reduced had significantly fewer DCV transport events (Table 1). Average DCV flux in KIF1A knockdown cells was significantly less ($0.83 \pm 0.23 \text{ min}^{-1}$; $p < 0.01$) than in cells expressing either empty vector or mouse KIF1A shRNA controls, where average DCV

flux was $4.10 \pm 0.58 \text{ min}^{-1}$ and $3.26 \pm 0.31 \text{ min}^{-1}$, respectively (Table 1). Average anterograde DCV velocities in knockdown cells were not significantly different compared to control cells ($1.25 \pm 0.07 \mu\text{m/s}$ and $1.43 \pm 0.09 \mu\text{m/s}$, respectively; Table 1). A small reduction in retrograde DCV velocity was observed in KIF1A shRNA cells relative to controls (1.30 ± 0.06 and $1.53 \pm 0.09 \mu\text{m/s}$, respectively, $p < 0.05$), however this velocity is still within the typical range of retrograde axonal transport velocities [37,4,21,13]. While there was no difference in retrograde run lengths between controls and KIF1A shRNA-expressing cells, a significant difference was observed in anterograde run length ($7.12 \pm 0.52 \mu\text{m}$ and $4.97 \pm 0.63 \mu\text{m}$, respectively, $p < 0.05$; Table 1). Finally, we observed a significant increase in the number of stationary objects in KIF1A knockdown cells, as compared to controls (Table 1).

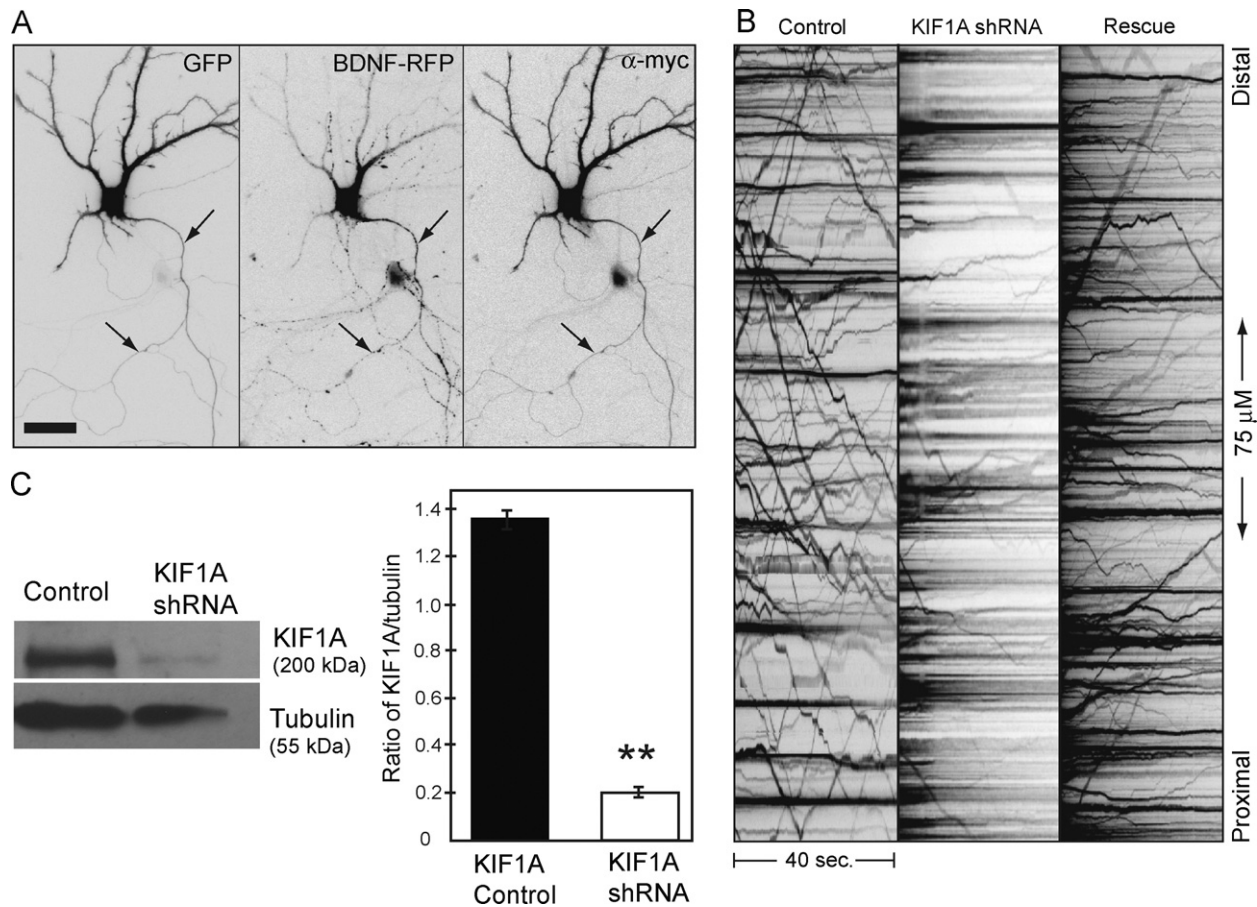


Fig. 2. Bidirectional transport of DCVs is significantly reduced in KIF1A knockdown neurons. (A) Fluorescence micrographs of a 9 DIV neuron expressing soluble GFP to confirm KIF1A shRNA expression, BDNF-RFP, and a myc-tagged KIF1A rescue plasmid. Triply transfected cells were allowed to express plasmids for 48 h prior to imaging. The axon is denoted by arrows. Inset scale bar: 50 μm (B) Example kymographs comparing transport of BDNF-RFP between control, shRNA, and KIF1A-rescue neurons (left to right). (C) Example immunoblots performed on neuronal lysates demonstrating knockdown of KIF1A. Similar results were obtained in control conditions, with either empty vector or shRNA against mouse KIF1A. Quantification of the knockdown of KIF1A is expressed as a ratio of KIF1A to tubulin expression. Control = 1.4 ± 0.08 ; shRNA = 0.2 ± 0.05 $^{**}p < 0.01$.

To rule out the possibility that our KIF1A knockdown results were due to off-target effects of shRNA expression, we assessed the ability of an shRNA-resistant form of KIF1A (KIF1A-rescue) to rescue DCV transport in neurons expressing KIF1A shRNA and either BDNF-RFP or NPY-RFP. Expression of KIF1A-rescue resulted in recovery of overall DCV flux (Fig. 2; Table 1). There was a reduction in retrograde flux compared to controls in this experiment, however KIF1A-rescue flux values are significantly greater than KIF1A shRNA treated cells ($p < 0.0001$).

To further demonstrate the specificity of our shRNA, we analyzed the movement of mitochondria, known to traffic independently of KIF1A, in neurons expressing KIF1A shRNA. The kinesin-1 family member, KIF5B, and another kinesin-3 family member, KIF1B, have been implicated in the transport of mitochondria [12]. We also analyzed the transport of the dendritically localized transferrin receptor (TfR), which is mediated by KIF16B or KIF5 [30,14]. The transport parameters of YFP-tagged mitochondria and GFP-TfR were similar in empty vector control and shRNA expressing cells (Table 1), indicating that the knockdown of KIF1A protein does not reduce their transport. To further confirm the specificity of KIF1A activity in DCV transport, we expressed a KIF5 dominant negative mutant that impairs the function of all three mammalian isoforms of KIF5 [19], and demonstrated that it had no significant effect on DCV flux ($89.14 \pm 11.03\%$ of control), yet as expected, reduces mitochondria transport in cultured cortical neurons (G. Rintoul, unpublished observation).

4. Discussion

Previous studies have implicated KIF1A in the transport of DCVs in mammalian neurons [24,3]. Here, using a combination of live-cell imaging and RNAi technology, we have shown a direct role for KIF1A in the microtubule-based transport of DCVs in axons of cultured rat hippocampal neurons. In addition, we provide evidence that KIF1A remains associated with DCVs during retrograde axonal transport, demonstrating that the DCVs retain molecular machinery readily competent of transport in either direction.

The proper transport of DCVs and their associated cargo is critical for normal neuronal function. In addition to the need for DCVs and their cargo to be transported to the appropriate subcellular sites, the time spent in transit is needed for the proteolytic cleavage of precursor molecules into their active forms [15]. KIF1A, which transports synaptic vesicle precursors [35], is also well suited for the transport of DCVs. KIF1A is a highly processive, fast motor with varied mechanisms for binding different cargos [12,18], similar to other motors implicated in axonal transport, such as KIF5 and dynein [18,32]. Based on data presented here and biochemical evidence presented by others [24], a strong case exists for KIF1A as the primary motor for DCV transport. We demonstrate that knockdown of KIF1A leads to a reduction in overall vesicle flux, including flux in the retrograde direction. This finding is consistent with data from *unc-104* mutants and supports the notion that a cooperative motor complex is present on DCVs [4], similar to mitochondria and

Table 1
Quantitative analysis of DCV, mitochondria, and TFR transport.

	Traffic values			% of control
	All events	Anterograde	Retrograde	All events
Flux (min⁻¹)				
Control	4.10 ± 0.58	2.11 ± 0.35	1.99 ± 0.28	100.00 ± 14.19
Mouse KIF1A RNAi	3.26 ± 0.31	1.56 ± 0.20	1.70 ± 0.17	79.53 ± 7.48
Rat KIF1A RNAi	0.83 ± 0.23 ^{**}	0.46 ± 0.14 ^{**}	0.37 ± 0.11 ^{**#}	20.31 ± 5.66 ^{**}
RNAi rescue	2.87 ± 0.22	1.67 ± 0.17	1.20 ± 0.11 [#]	70.07 ± 5.31
Mitochondria (control)	0.23 ± 0.04	0.11 ± 0.02	0.12 ± 0.02	100.00 ± 17.38
Mitochondria (RNAi)	0.28 ± 0.05	0.15 ± 0.02	0.13 ± 0.03	123.95 ± 20.22
TFR (control)	2.23 ± 0.50	0.98 ± 0.26	1.25 ± 0.26	100.00 ± 22.44
TFR (RNAi)	1.96 ± 0.35	0.99 ± 0.17	0.97 ± 0.18	87.74 ± 15.64
Velocity (μm/s)				
Control	1.49 ± 0.09	1.43 ± 0.09	1.53 ± 0.09	100.00 ± 5.83
Mouse KIF1A RNAi	1.38 ± 0.04	1.32 ± 0.04	1.41 ± 0.05	92.96 ± 2.84
Rat KIF1A RNAi	1.29 ± 0.06	1.25 ± 0.07	1.30 ± 0.06 [#]	86.46 ± 4.01
RNAi rescue	1.50 ± 0.06	1.48 ± 0.06	1.54 ± 0.08	100.63 ± 3.83
Mitochondria (control)	0.30 ± 0.07	0.26 ± 0.05	0.32 ± 0.09	100.00 ± 24.55
Mitochondria (RNAi)	0.26 ± 0.06	0.23 ± 0.04	0.28 ± 0.06	88.29 ± 18.56
TFR (control)	1.39 ± 0.05	1.39 ± 0.06	1.37 ± 0.08	100.00 ± 3.81
TFR (RNAi)	1.39 ± 0.24	1.32 ± 0.22	1.45 ± 0.26	100.37 ± 17.37
Run length (μm)				
Control	6.60 ± 0.47	7.12 ± 0.52	6.06 ± 0.47	100.00 ± 7.17
Mouse KIF1A RNAi	5.77 ± 0.24	5.49 ± 0.33 ⁺	5.72 ± 0.28	87.45 ± 3.62
Rat KIF1A RNAi	5.15 ± 0.50	4.97 ± 0.64 ^{**}	5.09 ± 0.47	78.06 ± 7.54
RNAi rescue	5.24 ± 0.52	5.75 ± 0.76	4.73 ± 0.47	79.37 ± 7.82
Mitochondria (control)	5.75 ± 0.46	5.78 ± 0.83	5.22 ± 0.59	100.00 ± 7.95
Mitochondria (RNAi)	8.76 ± 0.75 [†]	9.68 ± 0.92 ⁺	7.34 ± 0.87	152.36 ± 13.03 [†]
TFR (control)	4.43 ± 0.35	4.34 ± 0.44	4.48 ± 0.45	100.00 ± 7.97
TFR (RNAi)	3.88 ± 0.51	3.80 ± 0.49	3.97 ± 0.52	87.74 ± 11.43
Stationary objects (100 μm⁻¹)				
Control	22.01 ± 1.74			100.00 ± 7.92
Mouse KIF1A RNAi	24.97 ± 1.27			113.44 ± 5.79
Rat KIF1A RNAi	33.22 ± 3.01 [†]			150.90 ± 13.66 [†]
RNAi rescue	23.54 ± 1.92			106.92 ± 8.73

Control: n = 20 kymographs (20 cells, 1979 vesicles).

Mouse KIF1A RNAi: n = 44 kymographs (44 cells, 3395 vesicles).

Rat KIF1A RNAi: n = 27 kymographs (27 cells, 589 vesicles).

RNAi rescue: n = 19 kymographs (19 cells, 1151 vesicles).

Mitochondria (control): n = 14 kymographs (14 cells, 201 organelles).

Mitochondria (RNAi): n = 18 kymographs (18 cells, 300 organelles).

TFR (control): n = 19 kymographs (19 cells, 741 organelles).

TFR (RNAi): n = 23 kymographs (23 cells, 567 organelles).

^{**} p < 0.0001, when compared with control (all events).

[†] p < 0.05, when compared with control (all events).

^{**} p < 0.0001, when compared with anterograde control.

[†] p < 0.05, when compared with anterograde control.

^{**#} p < 0.0001, when compared with retrograde control.

[#] p < 0.05, when compared with retrograde control.

melanosomes [25,10]. Notably, recent work performed *in vitro* and in living cells provides a mechanistic explanation for motor coordination, by demonstrating that opposite polarity motors can be dependent on one another for activation [1,11].

Despite strong knockdown of KIF1A, modest DCV transport persists. This may be due to incomplete knockdown of KIF1A. Alternatively, other KIF1 family members, such as KIF1B or its multiple isoforms [23], or KIF1C or KIF1D, may functionally compensate for the loss of KIF1A. Although contentious (see Park et al. [24]), KIF5B has been proposed as a motor for BDNF-containing vesicles [7], and may also be recruited in the absence of KIF1A.

The retrograde movement of KIF1A in the axons of hippocampal neurons was first reported by Lee et al. [22]. This retrograde movement is notable, as axonal microtubules project from the cell body in a plus-end out orientation, suggesting that a plus-end motor like KIF1A is incapable of actively transporting in a retrograde fashion. KIF1A is also a retrograde cargo of the dynein complex [20]; however, our data represents the first evidence of bidirectional co-transport of KIF1A with DCVs. Although we do not find complete

overlap between KIF1A and DCVs, it is known that KIF1A also transports synaptic vesicle precursors [35]. Additionally, vesicles can be transported by as few as one or two motors [11,9]; thus, such small amounts of KIF1A-GFP attached to a DCV would be below the detection of standard fluorescent microscopy. Another explanation for incomplete overlap is that the DCVs have recruited sufficient endogenous KIF1A for efficient transport, and therefore do not associate further with expressed KIF1A-GFP. Nonetheless, these results indicate that in the axon, KIF1A and DCVs move in tandem in a bidirectional manner. This feature of organelle transport is considered important for obstacle avoidance [26], and to provide the cell with a readily mobile pool of vesicles, as described for ANF in *Drosophila* motor neurons [31].

A next step in understanding KIF1A-DCV interactions is to define the mechanism of motor-cargo binding. KIF1A contains multiple protein-protein interaction domains that facilitate differential cargo binding [18,32,34]. Additionally, Park et al. [24] demonstrated the formation of a complex between carboxypeptidase E and the dynactin complex, that then likely acts as a platform for KIF1A

binding. Yet, the exact mechanism for KIF1A binding to DCVs is not known. Another critical element in understanding mechanisms of DCV and axonal transport more generally is to define regulatory mechanisms for motor-cargo binding and motor processivity. Phosphorylation influences not only motor activity, but is also linked to axonal polarity and non-vesicular axonal transport, e.g., neurofilaments [2,6]. Importantly, aberrant phosphorylation of motor or motor-associated proteins occurs in Huntington's and Alzheimer's disease [6]. Thus, with identification of regulatory mechanisms that control the transport of BDNF and other DCV cargos, we will gain a better understanding of the molecular underpinnings of axonal transport in both healthy and diseased neurons.

Acknowledgements

This research was supported by grants from the Natural Science and Engineering Research Council, (NSERC; #327100-06), the Canadian Foundation for Innovation (CFI; #12793), and the Canadian Institutes of Health Research (CIHR; #90396). We thank David Kwinter for initiating these studies, Diana Hunter for her expert technical assistance, and Drs. Nick Inglis and Elisa Ramser for their critical reading of this manuscript. We also thank the Simon Fraser University Animal Care Services staff for their essential assistance in our experiments.

Appendix A. Supplementary data

Supplementary data associated with this article can be found, in the online version, at doi:10.1016/j.neulet.2011.01.018.

References

- [1] S. Ally, A.G. Larson, K. Barlan, S.E. Rice, V.I. Gelfand, Opposite-polarity motors activate one another to trigger cargo transport in live cells, *J. Cell Biol.* 187 (7) (2009) 1071–1082.
- [2] N. Arimura, K. Kaibuchi, Neuronal polarity: from extracellular signals to intracellular mechanisms, *Nat. Rev. Neurosci.* 8 (3) (2007) 194–205.
- [3] C.P. Arthur, C. Dean, M. Pagratis, E.R. Chapman, M.H. Stowell, Loss of synaptotagmin IV results in a reduction in synaptic vesicles and a distortion of the Golgi structure in cultured hippocampal neurons, *Neuroscience* 167 (1) (2010) 135–142.
- [4] R.V. Barkus, O. Klyachko, D. Horiuchi, B.J. Dickson, W.M. Saxton, Identification of an Axonal Kinesin-3 Motor for Fast Anterograde Vesicle Transport that Facilitates Retrograde Transport of Neuropeptides, *Mol. Biol. Cell* 19 (1) (2008) 274–283.
- [5] S. Cohen, M.E. Greenberg, Communication between the synapse and the nucleus in neuronal development, plasticity, and disease, *Annu. Rev. Cell Dev. Biol.* 24 (2008) 183–209.
- [6] K.J. De Vos, A.J. Grierson, S. Ackerley, C.C. Miller, Role of axonal transport in neurodegenerative diseases, *Annu. Rev. Neurosci.* 31 (2008) 151–173.
- [7] J.P. Dompierre, J.D. Godin, B.C. Charrin, F.P. Cordelieres, S.J. King, S. Humbert, F. Saudou, Histone deacetylase 6 inhibition compensates for the transport deficit in Huntington's disease by increasing tubulin acetylation, *J. Neurosci.* 27 (13) (2007) 3571–3583.
- [8] L.J. Goodman, J. Valverde, F. Lim, M.D. Geschwind, H.J. Federoff, A.I. Geller, F. Hefti, Regulated release and polarized localization of brain-derived neurotrophic factor in hippocampal neurons, *Mol. Cell. Neurosci.* 7 (3) (1996) 222–238.
- [9] S.P. Gross, Hither and yon: a review of bi-directional microtubule-based transport, *Phys. Biol.* 1 (1–2) (2004) R1–11.
- [10] S.P. Gross, M.C. Tuma, S.W. Deacon, A.S. Serpinskaya, A.R. Reilein, V.I. Gelfand, Interactions and regulation of molecular motors in *Xenopus melanophores*, *J. Cell Biol.* 156 (5) (2002) 855–865.
- [11] A.G. Hendricks, E. Perlson, J.L. Ross, H.W. Schroeder 3rd, M Tokito, E.L. Holzbaur, Motor coordination via a tug-of-war mechanism drives bidirectional vesicle transport, *Curr. Biol.* (2010).
- [12] N. Hirokawa, Y. Noda, Intracellular transport and kinesin superfamily proteins, KIFs: structure, function, and dynamics, *Physiol. Rev.* 88 (3) (2008) 1089–1118.
- [13] N. Hirokawa, R. Takemura, Molecular motors and mechanisms of directional transport in neurons, *Nat. Rev. Neurosci.* 6 (3) (2005) 201–214.
- [14] S. Hoepfner, F. Severin, A. Cabezas, B. Habermann, A. Runge, D. Gillyooly, H. Stenmark, M. Zerial, Modulation of receptor recycling and degradation by the endosomal kinesin KIF16B, *Cell* 121 (3) (2005) 437–450.
- [15] V. Hook, M.H. Metz-Boutigue, Protein trafficking to chromaffin granules and proteolytic processing within regulated secretory vesicles of neuroendocrine chromaffin cells, *Ann. N. Y. Acad. Sci.* 971 (2002) 397–405.
- [16] T.C. Jacob, J.M. Kaplan, The EGL-21 carboxypeptidase E facilitates acetylcholine release at *Caenorhabditis elegans* neuromuscular junctions, *J. Neurosci.* 23 (6) (2003) 2122–2130.
- [17] S. Kaech, G. Banker, Culturing hippocampal neurons, *Nat. Protoc.* 1 (5) (2006) 2406–2415.
- [18] D.R. Klopfenstein, R.D. Vale, The lipid binding pleckstrin homology domain in UNC-104 kinesin is necessary for synaptic vesicle transport in *Caenorhabditis elegans*, *Mol. Biol. Cell* 15 (8) (2004) 3729–3739.
- [19] Y. Konishi, M. Setou, Tubulin tyrosination navigates the kinesin-1 motor domain to axons, *Nat. Neurosci.* 12 (5) (2009) 559–567.
- [20] S.P. Koushika, A.M. Schaefer, R. Vincent, J.H. Willis, B. Bowerman, M.L. Nonet, Mutations in *Caenorhabditis elegans* cytoplasmic dynein components reveal specificity of neuronal retrograde cargo, *J. Neurosci.* 24 (16) (2004) 3907–3916.
- [21] D.M. Kwinter, K. Lo, P. Mafi, M.A. Silverman, Dynactin regulates bidirectional transport of dense-core vesicles in the axon and dendrites of cultured hippocampal neurons, *Neuroscience* 162 (4) (2009) 1001–1010.
- [22] J.R. Lee, H. Shin, J. Ko, J. Choi, H. Lee, E. Kim, Characterization of the movement of the kinesin motor KIF1A in living cultured neurons, *J. Biol. Chem.* 278 (4) (2003) 2624–2629.
- [23] M. Matsushita, R. Yamamoto, K. Mitsui, H. Kanazawa, Altered motor activity of alternative splice variants of the mammalian kinesin-3 protein KIF1B, *Traffic* 10 (11) (2009) 1647–1654.
- [24] J.J. Park, N.X. Cawley, Y.P. Loh, A bi-directional carboxypeptidase E-driven transport mechanism controls BDNF vesicle homeostasis in hippocampal neurons, *Mol. Cell. Neurosci.* 39 (1) (2008) 63–73.
- [25] A.D. Pilling, D. Horiuchi, C.M. Lively, W.M. Saxton, Kinesin-1 and Dynein are the primary motors for fast transport of mitochondria in *Drosophila* motor axons, *Mol. Biol. Cell* 17 (4) (2006) 2057–2068.
- [26] J.L. Ross, M.Y. Ali, D.M. Warshaw, Cargo transport: molecular motors navigate a complex cytoskeleton, *Curr. Opin. Cell Biol.* 20 (1) (2008) 41–47.
- [27] B. Sampo, S. Kaech, S. Kunz, G. Banker, Two distinct mechanisms target membrane proteins to the axonal surface, *Neuron* 37 (4) (2003) 611–624.
- [28] B.A. Scalettar, How neurosecretory vesicles release their cargo, *Neuroscientist* 12 (2) (2006) 164–176.
- [29] M.A. Schlager, C.C. Hoogenraad, Basic mechanisms for recognition and transport of synaptic cargos, *Mol. Brain* 2 (1) (2009) p25.
- [30] M.R. Schmidt, T. Maritzen, V. Kukhtina, V.A. Higman, L. Doglio, N.N. Barak, H. Strauss, H. Oschkinat, C.G. Dotti, V. Haucke, Regulation of endosomal membrane traffic by a Gadkin/AP-1/kinesin KIF5 complex, *Proc. Natl. Acad. Sci. U.S.A.* 106 (36) (2009) 15344–15349.
- [31] D. Shakiryanova, A. Tully, E.S. Levitan, Activity-dependent synaptic capture of transiting peptidergic vesicles, *Nat. Neurosci.* 9 (7) (2006) 896–900.
- [32] H. Shin, M. Wyszynski, K.H. Huh, J.G. Valtchanoff, J.R. Lee, J. Ko, M. Streuli, R.J. Weinberg, M. Sheng, E. Kim, Association of the kinesin motor KIF1A with the multimodular protein liprin- α , *J. Biol. Chem.* 278 (13) (2003) 11393–11401.
- [33] M.A. Silverman, S. Johnson, D. Gurkins, M. Farmer, J.E. Lochner, P. Rosa, B.A. Scalettar, Mechanisms of transport and exocytosis of dense-core granules containing tissue plasminogen activator in developing hippocampal neurons, *J. Neurosci.* 25 (12) (2005) 3095–3106.
- [34] X. Xue, F. Jaulin, C. Espenel, G. Kreitzer, PH-domain-dependent selective transport of p75 by kinesin-3 family motors in non-polarized MDCK cells, *J. Cell Sci.* 123 (Pt 10) (2010) 1732–1741.
- [35] Y. Yonekawa, A. Harada, Y. Okada, T. Funakoshi, Y. Kanai, Y. Takei, S. Terada, T. Noda, N. Hirokawa, Defect in synaptic vesicle precursor transport and neuronal cell death in KIF1A motor protein-deficient mice, *J. Cell Biol.* 141 (2) (1998) 431–441.
- [36] A. Yoshii, M. Constantine-Paton, Postsynaptic BDNF-TrkB signaling in synapse maturation, plasticity, and disease, *Dev. Neurobiol.* 70 (5) (2010) 304–322.
- [37] T.R. Zahn, J.K. Angleson, M.A. MacMorris, E. Domke, J.F. Hutton, C. Schwartz, J.C. Hutton, Dense core vesicle dynamics in *Caenorhabditis elegans* neurons and the role of kinesin UNC-104, *Traffic* 5 (7) (2004) 544–559.